Microwave photonic phase shifter with spectral separation processing using a linear chirped fiber Bragg grating

Wensheng Zhai (翟文胜), Xinlu Gao (高欣璐), Wenjing Xu (徐文静), Mingyang Zhao (赵明阳), Mutong Xie (谢牧彤), Shanguo Huang (黄善国)*, and Wanyi Gu (顾畹仪)

State Key Laboratory of Information Photonics and Optical Communications, Beijing University of Posts and Telecommunications, Beijing 100876, China

**Corresponding author: shghuang@bupt.edu.cn*

Received November 20, 2015; accepted January 25, 2016; posted online March 16, 2016

A stable and broadband microwave photonic phase shifter based on the combined use of a linear chirped fiber Bragg grating and optical single-sideband (OSSB) modulation is proposed and experimentally demonstrated. The quality of the radio frequency (RF) signal is improved by the spectral separation delay processing. The theoretical fundamentals of the scheme are explained and the phase shift can be controlled linearly by the wavelength of the light source. In the experiment, a full 360° phase shift with a 10 GHz bandwidth can be achieved and tuned dynamically, continuously, and stably.

OCIS codes: 060.3735, 060.4510, 060.5625.

doi: 10.3788/COL201614.040601.

A microwave photonic phase shifter is one of the essential components in microwave communication and radar systems, etc.[1,2]. It has attracted widespread attention owing to its large instantaneous bandwidth and wide range of adjustable phase shift compared with the conventional radio frequency (RF) phase shifter. Recently, various techniques of microwave photonic phase shifters have been reported, such as nonlinear effects[3,4], homodyne mixing techniques[5,6], vector sum techniques[7,8], and optical true time delay techniques[9,10]. For instance, the stimulated Brillouin scattering (SBS) processing method has obvious advantages, such as simple structure and easy realization[11,12]. In these schemes, the modulation sideband information is easily disturbed when processing the optical carrier and the sideband simultaneously, which may weaken the stability of the RF signal. The above problems also exist in some other schemes implemented using the optical phase modulator[13], which may bring down the feasibility for practical applications. In addition, the optical filter is applied and constructed by some schemes[14,15], which benefits the information stability with the free spectral range matching. While the sideband isolates from the optical carrier, it is beneficial for raising the modulation information stable transmission. In order to further fix the issue, the modulation sideband information should be protected so the noise interference can be efficiently suppressed in practical applications.

In this Letter, a microwave photonic phase shifter scheme for modulation information protection is proposed. It employed spectral separation processing but purely processing the carrier; the modulated information can be protected to realize the high quality of the RF signal transmission. In this approach, a dual drive Mach–Zehnder modulator (DD-MZM) implements the single sideband (SSB) modulation. The SSB signals are divided into two parts by an optical coupler, and then the sideband and the optical carrier pass through optical bandpass filters (OBPFs), respectively. In link1, the optical carrier is coupled into a linear chirped fiber Bragg grating (LCFBG) by an optical circulator and gets different time delays corresponding to different wavelengths. In link2, the sideband signal maintains a constant transmission. Then, the sideband and optical carrier are coupled by an optical coupler. The synthetic signals are fed to a photodetector (PD, Optilab, LR-30) by the polarization controller. With purely adding a time delay to the optical carrier, the experimental results demonstrate that the system implements a full 360° phase shift with a low power variation of less than 1.26 dB and a low phase deviation of less than 1.6°. The operational bandwidth of the RF signal is from 10 to 20 GHz. By analysis, this scheme can achieve a stable phase shift over a very wide bandwidth microwave signal.

Figure 1 schematically depicts the experimental setup of the proposed microwave photonic phase shifter based on a LCFBG[16], which can provide an ideal delay line with a large delay, wide bandwidth, and high reflectivity. The DD−MZM (FTM7921ER) with the high extinction ratio of about 20 dB was used to implement the SSB modulation[17].

An SSB signal is comprised of one sideband and one optical carrier. It can be expressed as

$$E_A(t) = A\{\exp(j\omega_c t + \varphi_c) + \gamma \exp[j(\omega_c + \omega_m)t + \varphi_m]\}, \tag{1}$$

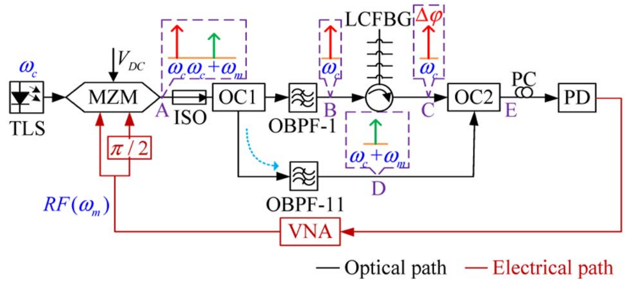

Fig. 1. Experimental setup of the proposed linear photonic RF phase shifter with the optical carrier delay processing. OC, optical coupler.

where A is the amplitude of the optical carrier, and γ is the modulation index. ω_c, ω_m, and $\omega_c + \omega_m$ are, respectively, the angular frequencies of the optical carrier, the microwave signal, and the upper sideband. Moreover, φ_c and φ_m are the initial phases of the optical carrier and sideband, respectively. Then, the SSB signal is launched into an optical coupler, and the sideband and optical carrier are separated by two OBPFs. So the optical carrier can be given by

$$E_B(t) = A\exp(j\omega_c t + \varphi_c). \quad (2)$$

As shown in Fig. 1, the optical carrier without any information is fed to the LCFBG by an optical circulator. Here, the optical carrier will get different time delays corresponding to the tunable wavelength with introducing an optical phase shift, which can be written as

$$E_C(t) = A\exp(j\omega_c t + \varphi_c - \Delta\varphi). \quad (3)$$

Along the axial orientation for the LCFBG at point Z, $\lambda(z) = 2n_{\text{eff}}(z)\cdot\Lambda(z)$ is the Bragg reflection wavelength, where $n_{\text{eff}}(z)$ is the effective refractive index and $\Lambda(z)$ is the period of the grating; $\tau(\lambda) = D\cdot(\lambda - \lambda_0) = D\cdot\Delta\lambda_c$ is the time delay, where D is the dispersion coefficient; $\Delta\lambda_c$ is the wavelength variation of the optical carrier. $\Delta\varphi(\Delta\varphi = 2\pi\Delta\tau/T = 2\pi D\Delta\lambda_c/T)$ is the phase shift, where T is the period. Notice that the optical carrier is not carrying any modulation information, and the phase noise is suppressed. Through the second optical coupler, the synthetic signal is given by

$$E_E(t) = A\{\exp(j\omega_c t + \varphi_c - \Delta\varphi) + \gamma\exp[j(\omega_c + \omega_m)t + \varphi_m]\}. \quad (4)$$

Finally, the phase-shifted RF signal is expressed as follows after the detection of the SSB signal in a PD:

$$V(t) \propto \cos(\omega_m t + \Delta\varphi), \quad (5)$$

where, $\Delta\varphi$ is the phase shift of the RF signal. Through theoretical analyses, the proposal can implement the stable phase shift over a very wide bandwidth microwave signal.

To illustrate the performance of the broadband and phase stability of the RF signal based on the LCFBG with spectral separation processing, the operational bandwidth of the RF signal is from 10 to 20 GHz.

Figure 2 shows that the optical spectra are measured by a high resolution optical spectral analyzer (AQ6370B). With an optimal signal-to-noise ratio (SNR), the powers of the optical carrier and sideband are reasonably controlled. The power of thr sideband is −11.5 dBm, and the power of the optical carrier is 0 dBm. The power of the optical carrier is 11.5 dBm higher than that of the sideband. Meanwhile, the response speed of the system can be improved by the optical carrier and the sideband harmoniously working, which can keep the optical carrier and sideband balanced and the optimal ratio is acquired. Therefore, the receiver sensitivity of the system is realized with an optimal SNR and a high stability.

Figure 3 depicts that the time delay curve presents a linear relationship with the wavelength varying by a dispersion loss analyzer (Agilent, 86038B). The wavelength range is from 1550.244 to 1551.244 nm, and the operational bandwidth of the RF signal is from 10 to 20 GHz. As shown in Fig. 3, employed LCFBG can implement the stable time delay over a very wide bandwidth RF signal, from 1550.044 to 1552.244 nm.

Figure 4(a) presents that different optical wavelengths have different time delays; the graphic data was collected utilizing a vector network analyzer (Agilent, N5242A). Figure 4(b) shows that the RF signal implements a full

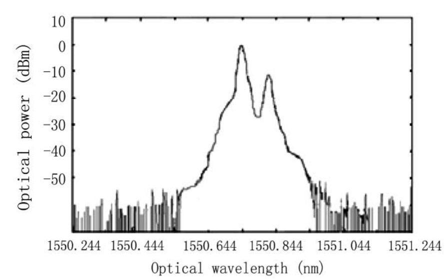

Fig. 2. Optical spectrum of an SSB modulated optical signal.

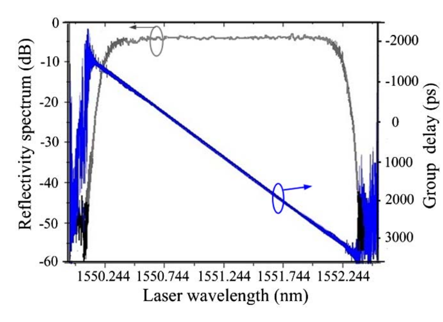

Fig. 3. Reflection spectrum and delay response of an optical signal about the LCFBG.

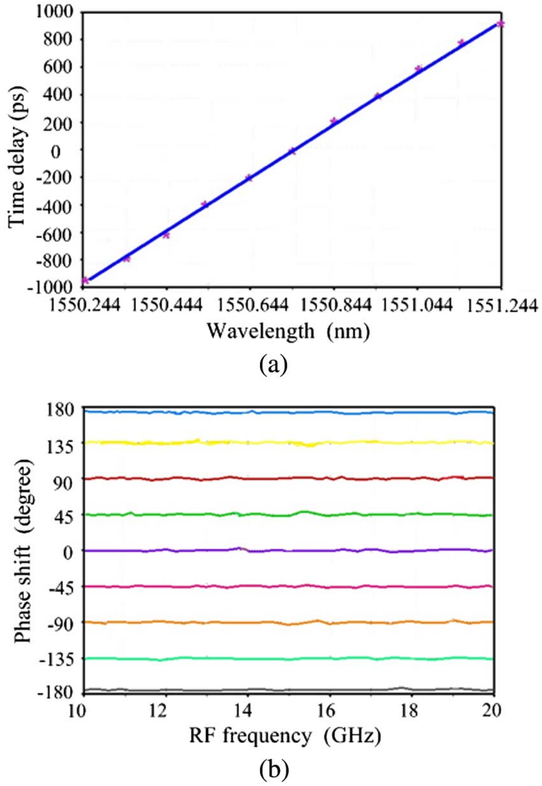

Fig. 4. Different wavelengths corresponding to different phase shifts. (a) Optical carrier time delay characteristics of different wavelengths and (b) RF signal phase shift over a frequency range from 10 to 20 GHz.

360° phase shift with a low phase deviation of less than 1.6° and an operational bandwidth from 10 to 20 GHz. As the LCFBG is employed to process the optical carrier rather than the sideband, which carries the modulation information, the ripples have neglibible effect on the generated phase shift.

Figure 5 describes the power spectra comparison of the RF signals whose frequency points are at 13 and 18 GHz with the optical carrier delay processing, and with the sideband delay processing, respectively, by a spectrum analyzer (RONO, 2688/2012). As shown in Figs. 5(a) and 5(c), the power spectra are polluted by noise owing to the sideband carrying information. The power brings out dispersive energy, leading to energy divergence. Eventually, the output RF signal might cause information distortion, which induces system instability. As shown in Figs. 5(b) and 5(d), the power spectra are more concentrated.

Figure 6 illustrates the phase noise spectra of the RF signals, whose frequency points are at 13 and 18 GHz with the sideband delay processing, and with the optical carrier delay processing, respectively. In Figs. 6(a) and 6(c), the phase noise spectra are seriously polluted by the fast fluctuation noise. The phase noise average value is approximate −105 dBc/Hz with the distribution of the frequency offset from 10 Hz to 100 kHz. Meanwhile, the curves are coarse and thick with lots

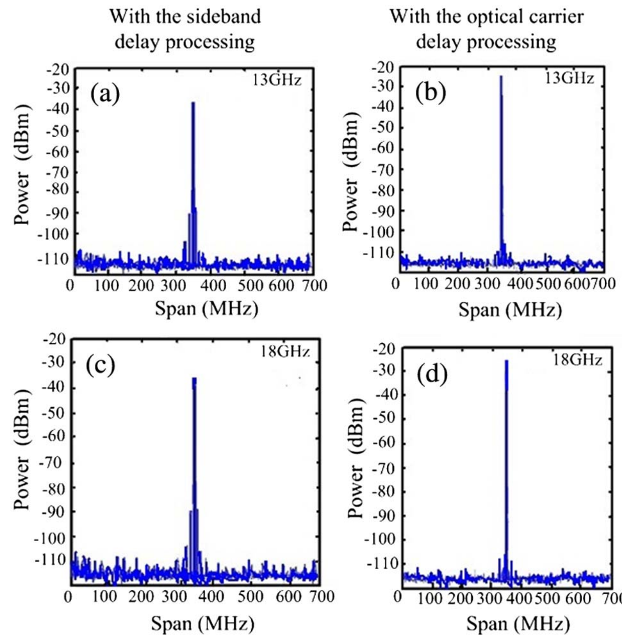

Fig. 5. Measured power spectra comparison of the transmitted RF signal at 13 and 18 GHz with the optical carrier delay processing and with the sideband delay processing, respectively.

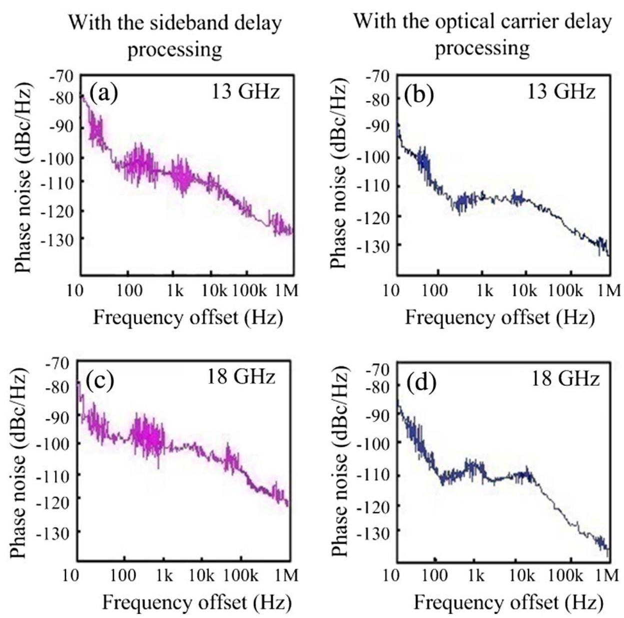

Fig. 6. Measured phase noise spectra comparison of the transmitted RF signal at 13 and 18 GHz with the sideband delay processing and with the optical carrier delay processing.

of burr. In Figs. 6(b) and 6(d), the phase noise is remarkably suppressed, with the phase noise average value approximately −115 dBc/Hz, and the distribution of the frequency offset is from 10 Hz to 10 kHz. Meanwhile, the curves are smooth and thin with a little burr. Through

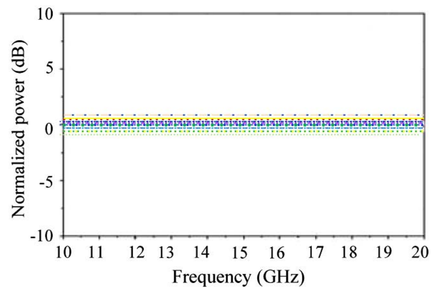

Fig. 7. Power of the phase-shifted microwave signal with the optical carrier delay processing when achieving different phase shifts.

analyses of experimental results, the phase noise has a negligible impact. Thus, this proposal is a promising option with optical carrier delay processing.

Figure 7 shows that there is less than 1.26 dB variation within the RF signal amplitude during the phase-shift processing, which is 0.38 dB slightly higher than the theoretical value with the stable running system. So the experimental results indicate that this is a promising proposal.

In conclusion, we propose a microwave photonic phase shifter scheme that employs spectral separation processing but purely processes the carrier;meanwhile, the modulated information can be protected to realize the high quality of the RF signal transmission. A full 360° phase shift with a 10 GHz bandwidth and high quality can be achieved and tuned dynamically, continuously, and stably. We plan to further investigate and optimize the phase resolution in future works.

This work was supported by the National "973" Program of China (No. 2012CB315604), the Natural Science Foundation of China (Nos. 61575028 and 61331008), the Program for New Century Excellent Talents in University (No. NCET-12-0793), the Beijing Nova Program (No. 2011065), and the Open Fund of Information Photonics and Optical Communications (Beijing University of Posts and Telecommunications).

References

1. J. Shen, G. Wu, L. Hu, W. Zou, and J. Chen, Opt. Lett. **39**, 2346 (2014).
2. C. Gao, S. Huang, J. Xiao, X. Gao, Q. Wang, Y. Wei, W. Zhai, W. Xu, and W. Gu, Chin. Opt. Lett. **13**, 010604 (2015).
3. Y. Dong, H. He, and W. Hu, Opt. Lett. **32**, 745 (2007).
4. W. Li, N. Zhu, and L. X. Wang, IEEE Photon. Technol. Lett. **23**, 1013 (2011).
5. S. S. Lee, A. H. Udupa, H. Erlig, H. Zhang, Y. Chang, C. Zhang, D. H. Chang, D. Bhattacharya, B. Tsap, W. H. Steier, L. R. Dalton, and H. R. Fetterman, IEEE Microw. Guided Wave Lett. **9**, 357 (1999).
6. H. Chen, Y. Dong, H. He, W. Hu, and L. Li, Opt. Lett. **34**, 2375 (2009).
7. X. Xue, X. Zheng, H. Zhang, and B. Zhou, Opt. Lett. **36**, 4641 (2011).
8. W. Liu, W. Li, and J. P. Yao, IEEE Photon. Technol. Lett. **25**, 1107 (2013).
9. H. Shahoei, M. Li, and J. Yao, J. Lightwave Technol. **29**, 1465 (2011).
10. Y. Wei, C. Yuan, S. Huang, X. Gao, J. Zhou, X. Han, and W. Gu, Chin. Opt. Lett. **11**, 100606 (2013).
11. A. Loayssa and F. J. Lahoz, IEEE Photon. Technol. Lett. **18**, 208 (2006).
12. M. Pagani, D. Marpaung, D.-Y. Choi, S. J. Madden, B. Luther-Davies, and B. J. Eggleton, Opt. Express **22**, 28810 (2014).
13. Z. Li, H. Shang, J. Li, C. Yu, X. Feng, B. Guan, and C. Lu, Opt. Commun. **297**, 55 (2013).
14. D. B. Adams and C. K. Madsen, J. Lightwave Technol. **26**, 2712 (2008).
15. J. Liu, N. Guo, Z. Li, C. Yu, and C. Lu, Opt. Lett. **38**, 4304 (2013).
16. Y. Chen, X. Feng, Z. Xu, and C. Liu, Chin. Opt. Lett. **13**, 123201 (2015).
17. Y. Zhang, F. Zhang, and S. Pan, Photon. Res. **2**, B80 (2014).